Ann Rheum Dis 85 (2026) 680–692

Contents lists available at ScienceDirect

Annals of the Rheumatic Diseases

journal homepage: https://www.sciencedirect.com/journal/annals-of-the-rheumatic-diseases

Systemic sclerosis

Identification of novel fibroblast subsets in diffuse cutaneous systemic sclerosis

Ann-Helen S Rosendahl[1,*], Anna Bornikoel[1], Isabel Zeinert[1], Lena Keufgens[2], Frederik Tellkamp[2], Niklas Kleinenkuhnen[3], Till Baar[3], Katrin Schönborn[1], Marcus Krüger[2,4], Achim Tresch[2,3], Bent Brachvogel[5], Beate Eckes[1], Pia Moinzadeh[6], Thomas Krieg[1,2,4,6]

[1] *Translational Matrix Biology, Faculty of Medicine, University of Cologne, Cologne, Germany*
[2] *Cologne Excellence Cluster on Cellular Stress Responses in Ageing-Associated Diseases (CECAD), University of Cologne, Cologne, Germany*
[3] *Institute of Medical Statistics and Computational Biology, Faculty of Medicine, University of Cologne, Cologne, Germany*
[4] *Center for Molecular Medicine (CMMC), University of Cologne, Cologne, Germany*
[5] *University Hospital for Pediatrics and Adolescent Medicine, Experimental Neonatology, Faculty of Medicine, University of Cologne, Cologne, Germany*
[6] *Department of Dermatology, University of Cologne, Cologne, Germany*

ARTICLE INFO

Article history:
Received 31 July 2025
Received in revised form 17 November 2025
Accepted 28 November 2025

ABSTRACT

Objectives: Systemic sclerosis (SSc) is an autoimmune-driven fibrotic disease, characterised by excessive extracellular matrix (ECM) deposition and fibroblast activation. Our study aimed to identify novel fibroblast subpopulations in SSc and determine their functional role.

Methods: We performed single-cell RNA sequencing on cultured dermal fibroblasts from healthy donors and patients with diffuse cutaneous SSc, verified selected, specific genes at the protein level and used siRNA knockdown experiments to provide evidence for a functional role of these proteins.

Results: SSc fibroblasts revealed high heterogeneity and in specific activated subsets strong upregulation of CD9 and four and a half LIM domain 1 (FHL1), previously described as a muscle-related protein. Overexpression of FHL1 and CD9 was also detected in fibroblast subsets in patient skin. CD9 was associated with the regulation of *FHL1* expression. Downmodulation of *FHL1* in primary skin fibroblasts correlated with downregulation of the vestigial-like family member 3 (*VGLL3*) gene, which is known to be expressed in myofibroblasts in a stiff and fibrotic environment and to upregulate collagen synthesis. Further, VGLL3 was confirmed to be upregulated in SSc donor skin.

Conclusions: Our study identified novel fibroblast subsets in SSc, characterised by CD9 and/or FHL1 upregulation. The data indicate a functional role of FHL1 in fibroblasts and its involvement in the regulation of ECM production and provide a new mechanistic link to VGLL3 regulation. Our findings suggest new avenues for therapeutic exploration targeting the perpetuating fibroblast activation by the fibrotic environment.

*Correspondence to Dr. Ann-Helen S Rosendahl, PhD.
E-mail address: ann-helen.rosendahl@hus.fi (A.-H.S. Rosendahl).
Handling editor Josef S. Smolen.

https://doi.org/10.1016/j.ard.2025.11.027

0003-4967/© 2025 The Author(s). Published by Elsevier B.V. on behalf of European Alliance of Associations for Rheumatology (EULAR). This is an open access article under the CC BY license (http://creativecommons.org/licenses/by/4.0/)

WHAT IS ALREADY KNOWN ON THIS TOPIC

- Systemic sclerosis (scleroderma) is a chronic fibrosing disease that has a major impact on the quality of life of the patients.
- Vascular damage and an inflammatory reaction lead to the activation of fibroblasts and the excessive deposition of connective tissue.
- Fibroblasts are now known to have many different functions; they produce extracellular matrix material, but also play a key role in the regulation of inflammation.
- Several populations of fibroblasts have already been described in normal and fibrotic skin. These are thought to differ in their function.

WHAT THIS STUDY ADDS

- In this study, we describe novel populations of fibroblast subsets in scleroderma skin, and we characterise their gene and protein expression profiles and demonstrate that these populations are also detected in the involved skin of the patients and in fibrotic murine skin.
- The data support a functional role of these proteins in the ongoing fibrosing reaction.

HOW THIS STUDY MIGHT AFFECT RESEARCH, PRACTICE OR POLICY

- We provide data for the characterisation of unique, activated fibroblast populations.
- These populations can be identified in the skin of the patients providing new biomarkers for activated fibroblasts.
- In addition, these described genes/proteins represent potential targets for new therapeutic approaches to limit fibrosing processes. Systemic sclerosis might represent a model for fibrotic diseases in general.

INTRODUCTION

Scleroderma or systemic sclerosis (SSc) is a chronic autoimmune-driven fibrotic disease affecting the skin and many internal organs; it can occur in a diffuse cutaneous SSc (dcSSc) and a limited cutaneous SSc (lcSSc) subset [1,2]. Although the early pathophysiology involves initial vascular damage and a subsequent inflammatory reaction, the final activation of fibroblasts leads to the characteristic excessive deposition of extracellular matrix (ECM) and tissue damage.

Fibroblasts are a heterogeneous cell type, and several subsets in normal and fibrotic skin can be differentiated [3–5]. They play a fundamental role in the structural support of tissues by producing ECM proteins, but also secrete cytokines and growth factors that act in autocrine and paracrine fashions. They are crucial for ensuring tissue homeostasis, modulate inflammatory responses and are key players in all tissue repair processes [6,7].

Single-cell transcriptomic analyses (single-cell RNA sequencing [scRNA-seq]) revealed details about heterogeneity of fibroblasts in sclerodermatous skin [8–10]. However, many of these studies are descriptive and it remains unclear whether these cells have a causal relationship to the ongoing pathogenetic events. It should also be emphasised that the heterogeneity of cells characterised by transcriptome analysis at a given time point does not necessarily define stable subsets of fibroblasts but may just reflect a particular dynamic cellular state. In addition, many of these recently published investigations were derived from cells released by enzymatic dissociation of rigid fibrotic tissue, a procedure that could lead to damage and loss of certain sensitive or fragile cell populations and therefore result in subsequent bias.

To overcome some of these restrictions, we concentrated on an alternative approach and used bulk fibroblast cultures obtained from skin biopsies of patients with SSc as described previously [11–13]. Using scRNA-seq analysis, this strategy allowed us to identify fibroblast subsets with a stable phenotype after several cell divisions. We then validated the gene expression by determining protein levels in fibroblast cultures and directly in patient tissue. We here describe new unique subsets, characterised by induced expression of CD9 and the four and a half LIM domain protein (FHL) 1, respectively [14,15]. We also identify these subsets in patient skin and in a bleomycin-induced fibrosis model in mice and propose a functional role of these proteins. Finally, we show that induced expression of CD9 and FHL1 is associated with the induction of vestigial-like family member 3 (VGLL3), a transcriptional cofactor known to induce ECM production [16].

METHODS

Study design

Scleroderma is a rare, still incurable disease. Our study was conducted to find possible new biomarkers that could aid in early diagnosis and open new treatment avenues. Examining the transcriptome of patient-derived cultured fibroblasts compared to healthy controls by scRNA-seq, we identified markers overexpressed in specific fibroblast subsets, including *CD9* and *FHL1*. We confirmed our results by western blot (WB) or Fluorescence-Activated Cell Sorting as well as immunofluorescent (IF) staining using fibroblasts from the same patients/controls and skin sections from patients with SSc and controls. For functional analysis, we performed knockdown experiments using siRNAs for *CD9* and *FHL1* in human fibroblasts, examining both the transcriptome and secretome. In addition, we employed an experimentally induced fibrosis model in mice to correlate CD9 and FHL1 expression with fibrotic conditions. The number of independent experiments (biological replicates, n) is indicated in each figure legend; no outliers were removed for statistical analysis.

Study population

Patient and control samples used in this study were age- and sex-matched (female or male) (Supplementary Table S1). All patients included in the scRNA-seq analysis were diagnosed with dcSSc.

Detailed descriptions of all materials and methods are provided in the Supplementary Materials [17–23].

Initiation of primary dermal fibroblast cultures

4 mm skin biopsies were obtained from study patients after informed consent. Primary dermal fibroblasts were obtained by outgrowth from the skin explants and cultured in Dulbecco's Modified Eagle Medium (Gibco Invitrogen, 41965-039) with 100 U/mL penicillin, 100 μg/mL streptomycin (Sigma, P0781), 2 mM L-glutamine (Biozym, 882027) 50 μg/mL Na-ascorbate (Sigma-Aldrich, A4034), and 10% fetal calf serum (Gibco, 10270-106) in 5% CO_2 at 37°C, harvested and analysed in passage 2-5.

Study approval

Skin biopsies were obtained from female and male healthy individuals or patients with scleroderma (SSc) after written consent and with approval of the local ethics committee (Ethics committee of the medical faculty of University of Cologne, 21-1072). The study was conducted in accordance with the criteria set by the Declaration of Helsinki.

Data and materials availability

All data generated during this study are included in this published article (and its supplementary information files). The RNA sequencing data were deposited in National Center for Biotechnology Information/Gene Expression Omnibus under the following accession numbers: scRNAseq—GSE294431, siRNA HPF Bulk—GSE294430 and CD9 MEF Bulk—GSE294429. The proteomics data have been deposited in PRoteomics IDEntifications Database (PRIDE) with the following accession numbers: Secretome—PXD062591 and proteome—PXD062597. Additional detailed information is available from the corresponding authors on request.

RESULTS

Fibroblasts were grown from dermal tissue explants, obtained from 4 patients with early diffuse cutaneous SSc [24] and 4 age-matched healthy controls (Supplementary Table S1). After 4 passages, we investigated these confluent fibroblast cultures by scRNA-seq analysis.

SSc dermal fibroblasts show altered transcriptional signatures and increased heterogeneity

We performed scRNA-seq on 37,343 cultured dermal fibroblasts from biopsies of 4 healthy donors (19,083 cells) and 4 patients with SSc (18,260 cells) (Supplementary Table S2). Unsupervised uniform manifold approximation and projection clustering (Louvain algorithm, resolution 0.28, see also Supplementary Table S3) identified 10 distinct fibroblast clusters (Fig 1A), with a clear separation between SSc and control fibroblasts (Fig 1B). Control fibroblasts primarily grouped into 2 major clusters (Fig 1B,C, Supplementary Fig S1), whereas the transcriptional signature of SSc fibroblasts displayed greater diversity (Fig 1B,C) including clusters 3 (IGFBP4^{hi}), 5 (POSTN^{hi}), 6 (MMP3^{hi}), 7 (SFRP1^{hi}), and 10 (FHL1^{hi}). Cluster 3, the largest of the SSc-specific clusters (28%), expressed genes involved in inflammation, fibroblast functions, and fibrosis (Fig 1B,C, Supplementary Table S4). Over 17% of the SSc-associated fibroblasts were found in cluster 5, with upregulated genes associated with fibrotic activity (Fig 1B,C, Supplementary Table S4). Cluster 6 (~14% of SSc fibroblasts) showed enrichment for genes involved in Bone Morphogenetic Protein signalling (BMP) signalling (Fig 1B,C, Supplementary Fig S2A, Supplementary Table S4). Genes in cluster 7 (12% of SSc fibroblasts) showed enrichment for response to oestrogen, and negative regulation of kinase and transferase activity (Fig 1B,C, Supplementary Fig S2B, Supplementary Table S4). Cluster 10 (FHL1^{hi}) was a small SSc-specific cluster (0.87%) with genes involved in muscle organ development, muscle cell differentiation, ECM, and extracellular structure organisation (Fig 1B,C, Fig 2B,C, Supplementary Fig S2C, Supplementary Table S4) indicating a special role of these fibroblasts for ECM deposition and remodelling.

Next, we asked if we could identify published marker genes of fibroblast clusters in our dataset. Papillary fibroblasts have been shown to be DPP4^{+}/ATXN1^{-}, while reticular fibroblasts mostly express PDPN and ATXN1 [3,4]. Our scRNA-seq data did

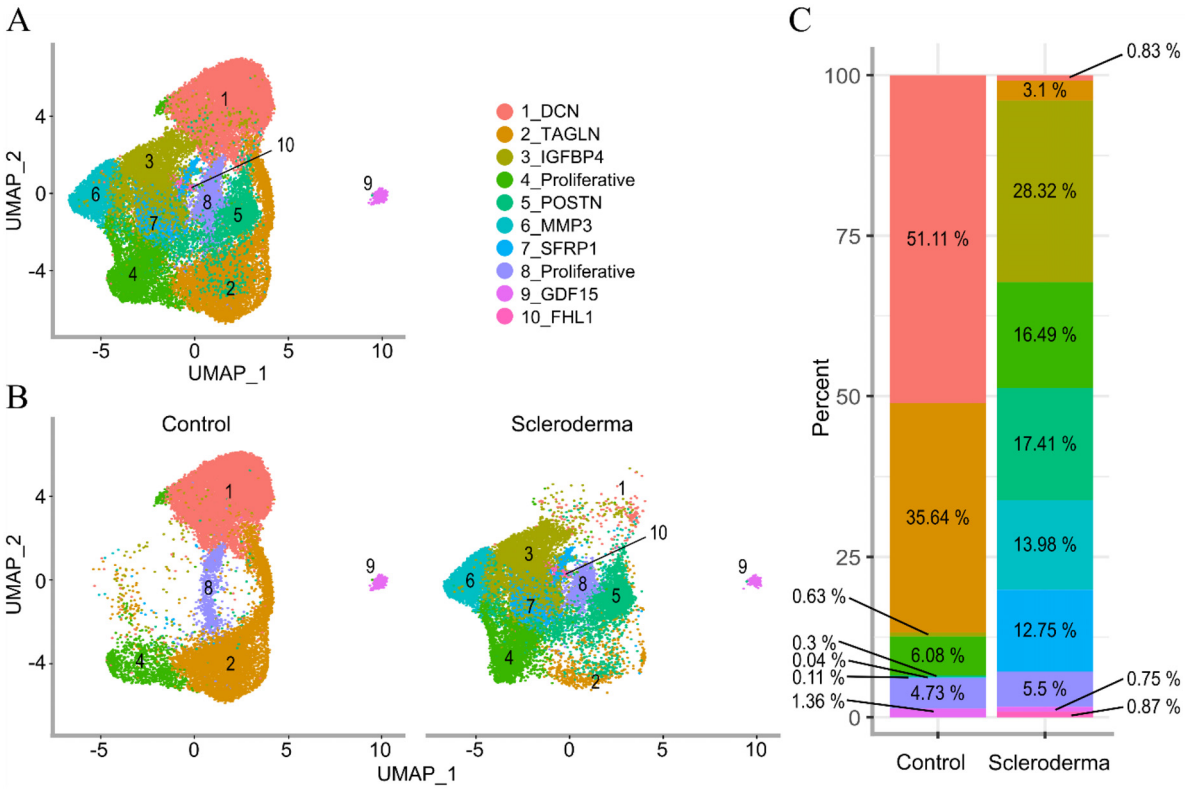

Figure 1. ScRNA-seq analysis of human dermal fibroblasts from 4 healthy control donors and 4 individuals with dcSSc. (A) UMAP representation of dermal fibroblasts processed from all 4 healthy controls and 4 samples obtained from patients with dcSSc, identified by marker genes. (B) Separated UMAP representation of all dermal fibroblasts processed from 4 healthy controls (left) and from 4 dcSSc fibroblast samples (right). dcSSc-specific clusters were clusters 3, 5, 6, 7, and 10. (C) Percentage of each cluster of control fibroblasts (left) and SSc fibroblasts (right). Colours of clusters in the UMAP (A, B) and the bar plot (C) correlate to the colours of the clusters 1–10, identified by marker genes. dcSSc, diffuse cutaneous systemic sclerosis; UMAP, Uniform Manifold Approximation and Projection; *DCN*, Decorin; *TAGLN*, Transgelin; *IGFBP4*, Insulin Like Growth Factor Binding Protein 4; *POSTN*, Periostin; *MMP3*, Matrix Metallopeptidase 3; *SFRP1*, Secreted Frizzled Related Protein 1; *GDF15*, Growth Differentiation Factor 15; *FHL1*, four and a half LIM domain 1; scRNA-seq, single-cell RNA sequencing; SSc, systemic sclerosis.

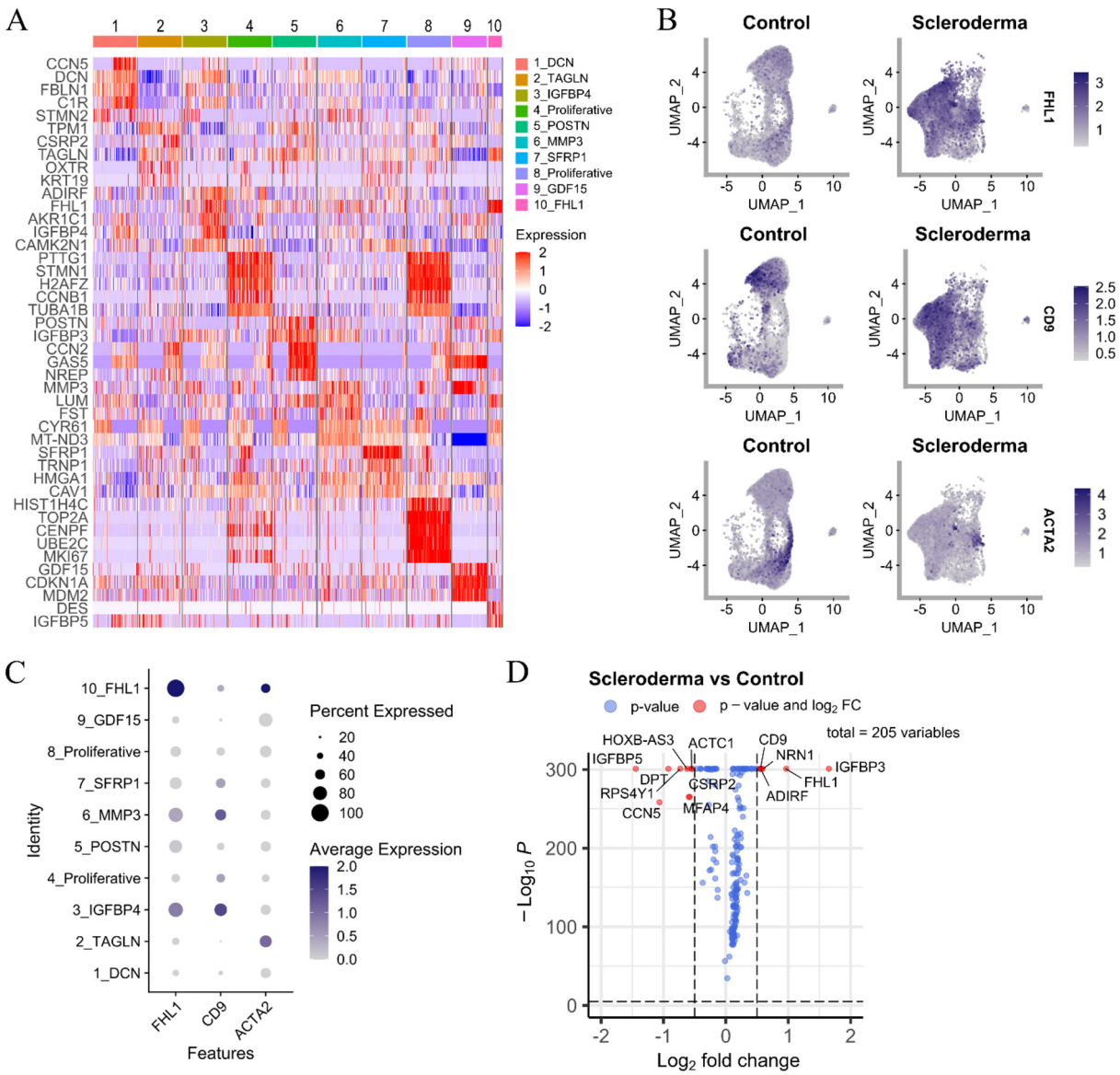

Figure 2. ScRNA-seq analysis of DEGs in fibroblasts obtained from patients with dcSSc compared to controls. (A) Heat map of scaled gene expression data for the top 5 DEGs for each cluster. (B) Feature plots of selected genes: *FHL1*, *CD9*, and *ACTA2*. Each dot represents a cell; the colour intensity of the dots correlates with increased expression. (C) Dot plot of selected genes: *FHL1*, *CD9*, and *ACTA2*. The size of the dot indicates the percentage of cells per cluster expressing the gene. The intensity of the colour shade of each dot correlates with the scaled average expression intensity in these cells. (D) Volcano plot of the most upregulated and downregulated genes in the SSc dermal fibroblasts when compared to control fibroblasts. Red dots indicate the significant genes that have an adjusted *P* value <.05 and that have a log2FC greater than .5. Significant genes are all labelled in the figure. DEGs, differentially expressed gene(s); dcSSc, diffuse cutaneous systemic sclerosis; *FHL1*, four and a half LIM domain 1; *ACTA2*, Actin Alpha 2; scRNA-seq, single-cell RNA sequencing; UMAP, Uniform Manifold Approximation and Projection.

not identify a clear pattern of these typical papillary or reticular markers (Supplementary Fig S3A,B). *DPP4* and *ATXN1* were expressed to some extent in all clusters, while *PDPN* was mostly expressed in control cluster 1 (DCN^{hi}) and SSc cluster 3 (IGFBP4^{hi}) (Supplementary Fig S3A,B). The same was found for other papillary fibroblast marker genes, such as *APCDD1*, *HSPB3*, and *WIF1*, as well as reticular fibroblast marker gene *CD36* [5]. We saw higher expression levels of *APCDD1* and *HSPB3* in cluster 3 (IGFBP4^{hi}), but again, no clear separation between reticular and papillary fibroblasts was detected (Supplementary Fig S3B).

However, in cluster 1, we identified expression of *SFRP2* (Supplementary Fig S3B), which together with *DPP4* marks a major fibroblast population in human skin [8] (Supplementary Fig S3A,B). In several of our clusters, we identified genes that were reported to correlate with the severity of SSc, such as *COMP* and *THBS1*, *CTGF*, *TNC*, *THY1*, *CDH11*, and *CCL2* [9] (Supplementary Fig S3C). These genes were found to some extent in all our fibroblast cultures but no clear differences were seen between SSc and controls.

Specific SSc fibroblast clusters reveal increased expression of FHL1 *and* CD9

The most striking observation was significantly increased *FHL1* expression in SSc fibroblasts, particularly in cluster 3 (IGFBP4^{hi}) and 10 (FHL1^{hi}), and to a lesser extent in cluster 6 (MMP3^{hi}) (Fig 2A-D). *FHL1* expression is highly abundant in muscle tissue [25], but has been found at low levels in multiple other tissues, such as heart, lung, and testis, but also in fibroblasts [14,26]. Its function in fibroblasts, however, has remained unknown. In cluster 10 (FHL1^{hi}), 100% and in clusters 3 (IGFBP4^{hi}) and 6 (MMP3^{hi}),

about 80% of the fibroblasts expressed *FHL1* at a high level (Fig 2C). These clusters were highly specific to SSc.

A second key observation was that we found an overall significant upregulation of *CD9* in our SSc-derived fibroblasts (Fig 2B-D). In our data, ~70% of the cells in cluster 3 (IGFBP4^{hi}) and ~60% of the fibroblasts in cluster 6 (MMP3^{hi}) expressed *CD9* at a high level (Fig 2C).

In cluster 10 (FHL1^{hi}), we further saw increased expression of profibrotic and ECM-related genes, such as *TAGLN*, *LUM*, *IGFBP5*, and *MFAP5*, but also muscle-related genes, such as *SYNPO2* and *MYL9* (Fig 2A, Supplementary Table S4). In addition, ~60% of the fibroblasts in the small profibrotic cluster 10 expressed smooth muscle α-2 actin (*ACTA2*; α-SMA). Even though *ACTA2* expression intensity was high in these cells, the fibroblasts did not cluster together with the other *ACTA2*$^{+}$ (myo)fibroblasts in clusters 2 and 5 (Fig 2B,C).

Cluster 3 (IGFBP4^{hi}) and 6 (MMP3^{hi}) expressed *FHL1* and *CD9* but lacked *ACTA2* expression (Fig 2B,C). *CD9* expression was also seen at a moderately high level in ~50% of the fibroblasts in clusters 7 (SFRP1^{hi}) and 4 (proliferative) with a discernible *FHL1* or *ACTA2* expression (Fig 2B,C).

High expression of *CD9* and *FHL1* genes in SSc was characteristic of SSc and prompted us to (i) validate these data at the protein level, (ii) search for expression of CD9 and FHL1 *in vivo* in patient skin, and (iii) demonstrate the functional relevance of these proteins.

Validation of increased FHL1 and CD9 protein in fibroblast cultures and patients with SSc

Next, we analysed several fibroblast cultures from controls and patients with SSc (6 independent biological replicates) by WB. These data clearly demonstrate that FHL1 protein amount was significantly increased in SSc fibroblasts *in vitro* (Fig 3A,B). The relative FHL1 protein amount in SSc fibroblasts was more than 4 times higher than in controls (Fig 3B). We also investigated fibroblasts from lcSSc samples, in which the clinical fibrosis was considerably less prominent. These samples only showed a slight increase in FHL1 (Fig 3B). IF staining confirmed FHL1 expression in many more SSc-derived fibroblasts in monolayer culture compared to controls (Fig 3C,D). Some cells in the SSc cultures showed markedly higher expression

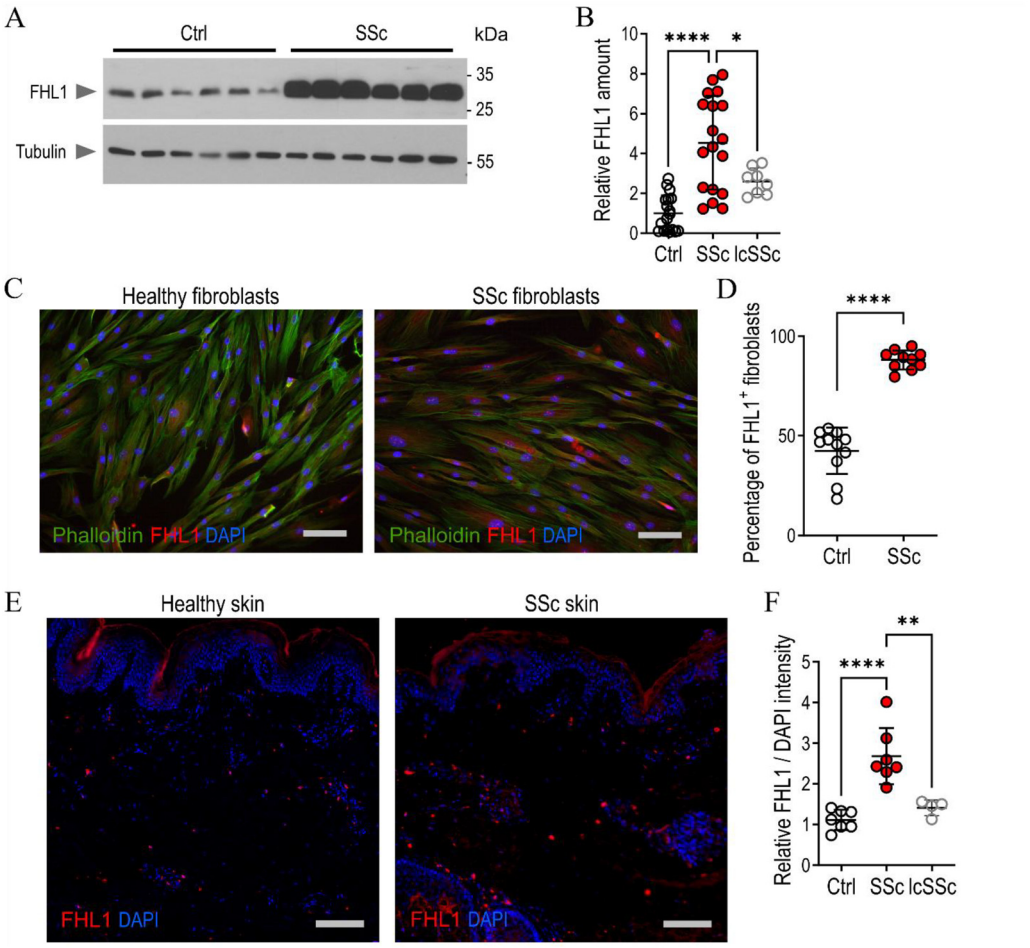

Figure 3. FHL1 protein amount is increased in specific subsets of SSc fibroblasts. (A) Representative western blot staining of FHL1 and β-tubulin in fibroblasts obtained from controls and patients with dcSSc. (B) Corresponding quantification from primary human dermal fibroblasts derived from healthy control skin, dcSSc skin and lcSSc skin (N = 18/18/8 independent samples or 6 Ctrl/6 SSc/4 patients with lcSSc, *P* values calculated with one-way ANOVA). (C) Representative IF staining of DAPI (blue), phalloidin (green) and FHL1 (red) in human healthy (left) and dcSSc fibroblasts (right) and (D) quantification of FHL1 positive fibroblasts (N = 11/12 measured images or 2 Ctrl/2 SSc patients; *P* values calculated with Welch's t-test, two-tailed). (E) IF staining of DAPI (blue) and FHL1 (red) in human healthy skin (left) and dcSSc skin (right). (F) Quantification of IF staining intensity of FHL1 normalised to cell number (DAPI) in human healthy, dcSSc, and lcSSc dermis. Data shown as relative values compared to control (N = 7 Ctrl/7 dcSSc /4 lcSSc donors, *P* values calculated with one-way ANOVA). **** $P \leq .0001$, ** $P = .0013$, * $P = .0166$; data shown as mean ± SD. Scale bar = 100 µm. ANOVA, analysis of variance; Ctrl, control; FHL1, four and a half LIM domain 1; IF, immunofluorescent; DAPI, 4',6-diamidino-2-phenylindole; dcSSc, diffuse cutaneous systemic sclerosis; lcSSc, limited cutaneous systemic sclerosis; SSc, systemic sclerosis.

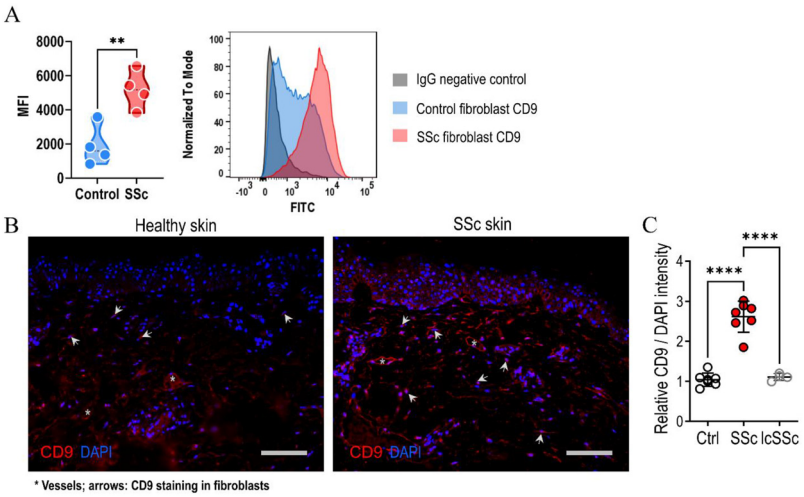

Figure 4. CD9 protein amount is increased in fibroblasts obtained from patients with dcSSc. (A) FACS analysis of CD9 staining in fibroblasts obtained from patients with dcSSc compared to control shown as violin plots. MFI = mean fluorescence intensity, N = 4 Ctrl/4 SSc donors; ** P = .0074, quantified with unpaired t-test, two-tailed. (B) IF staining of DAPI (blue) and CD9 (red) in human healthy (left) and dcSSc skin (right). (C) Quantification of CD9 staining intensity normalised to DAPI in human healthy, dcSSc, and lcSSc dermis. Data shown as relative values compared to control. N = 7 Ctrl/ 7 SSc/4 lcSSc donors; **** $P \leq .0001$, P values calculated with one-way ANOVA; data shown as mean ± SD. Scale bar = 100 μm. ANOVA, analysis of variance; Ctrl, control; FACS, Fluorescence-Activated Cell Sorting; dcSSc, diffuse cutaneous systemic sclerosis; IF, immunofluorescent; lcSSc, limited cutaneous systemic sclerosis; DAPI, 4',6-diamidino-2-phenylindole; FITC , Fluorescein Isothiocyanate; IgG, Immunoglobulin G.

than others. Notably, IF staining of skin biopsies obtained from patients with dcSSc also revealed significantly increased FHL1 expression, observed in many—but not all—fibroblasts (Fig 3E, F). The relative levels of FHL1 protein in the dermis of SSc skin, normalised to cell number, were up to 2.5 times higher than in healthy donor skin (Fig 3F). In contrast, in our lcSSc samples, we could only detect a slight increase in the intensity of FHL1 staining (Fig 3F).

In addition, we determined CD9 protein levels in dermal SSc fibroblasts. Flow cytometry of primary fibroblasts revealed a significant increase in CD9^{hi} fibroblasts in SSc vs control cultures (Fig 4A). Strikingly, significantly increased CD9 protein was also found *in vivo* in the dermis of skin biopsies obtained from patients with dcSSc (Fig 4B,C). The relative CD9 protein levels in SSc skin, quantified in the dermis only, were about 2.5 times higher than in healthy donor skin (Fig 4C). In contrast, we could not detect clear differences in the CD9 staining between control and lcSSc samples (Fig 4C). Of note, there was also increased CD9 staining of keratinocytes in the SSc biopsies (Fig 4B). To demonstrate the association of CD9 and FHL1 expressing fibroblast subsets with the development of fibrosis, we employed an independent system, the bleomycin-induced fibrosis in mice, which demonstrated that CD9- and FHL1-expressing fibroblasts are induced with the development of a fibrotic reaction upon injection of bleomycin into the dermis (Fig 5).

Loss of FHL1 *and* CD9 *from fibroblasts negatively impacts ECM deposition*

The striking upregulation of FHL1 and CD9 at both the transcript and protein levels in SSc fibroblast cultures obtained from patients with dcSSc and skin biopsies prompted us to investigate potential functional consequences. We therefore treated primary dermal fibroblasts from healthy donors with siRNAs targeting *FHL1* using siRNA against *Renilla reniformis* luciferase (*RLuc*) as a control. *FHL1* siRNA treatment resulted in a significant downregulation of *FHL1* expression (log2FC of −4.86; Supplementary Fig S4A,B) and fibroblasts also revealed a significant downregulation of genes associated with ECM or in fibrosis such as transforming growth factor beta-induced protein (*TGFBI*) (an ECM component involved in ECM organisation and pulmonary fibrosis [27]), Reticulocalbin 3 (*RCN3*) (involved in pulmonary fibrosis and activating fibroblasts [28]), collagen V α1 chain (*COL5A1*) (an ECM component required for correct assembly of fibril-forming collagens [29]), *VGLL3*, nidogen 2 (*NID2*) and prolyl 4-

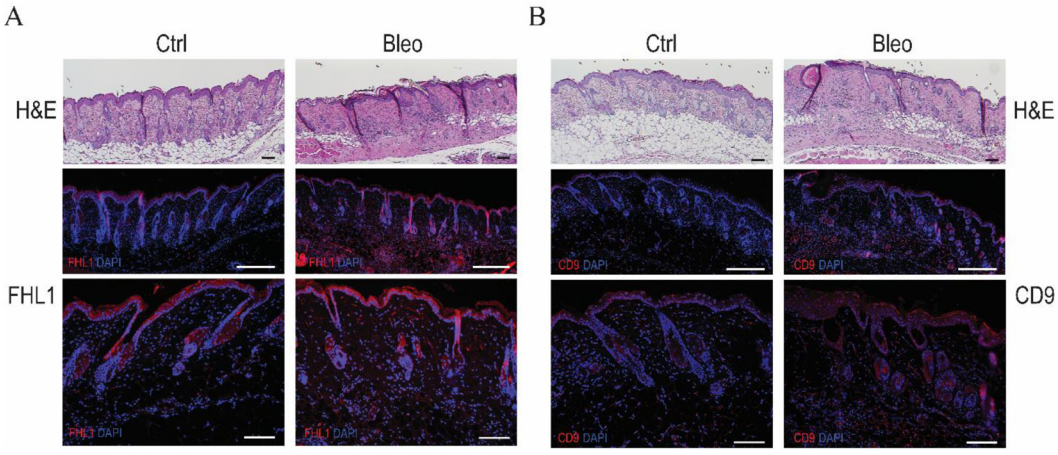

Figure 5. Increased amounts of FHL1 and CD9 protein in fibrotic skin of mice. Skin fibrosis was induced by intradermal bleomycin injections in mice. Sections were evaluated by histology (haematoxylin and eosin [H&E]) and IF staining of control (Ctrl) and fibrotic (Bleo) skin lesions. (A) H&E and IF staining of FHL1 (red); (B) H&E and IF staining of CD9 (red) of control (left) and fibrotic (right) skin. Nuclei are marked by DAPI (blue). Upper IF panels show overviews and bottom panels show higher magnification. Scale bars: 100 μm in H&E, 300 μm in IF overviews (top panels), and 100 μm in higher magnification images (bottom panels). FHL1, four and a half LIM domain 1; IF, immunofluorescent; DAPI, 4',6-diamidino-2-phenylindole.

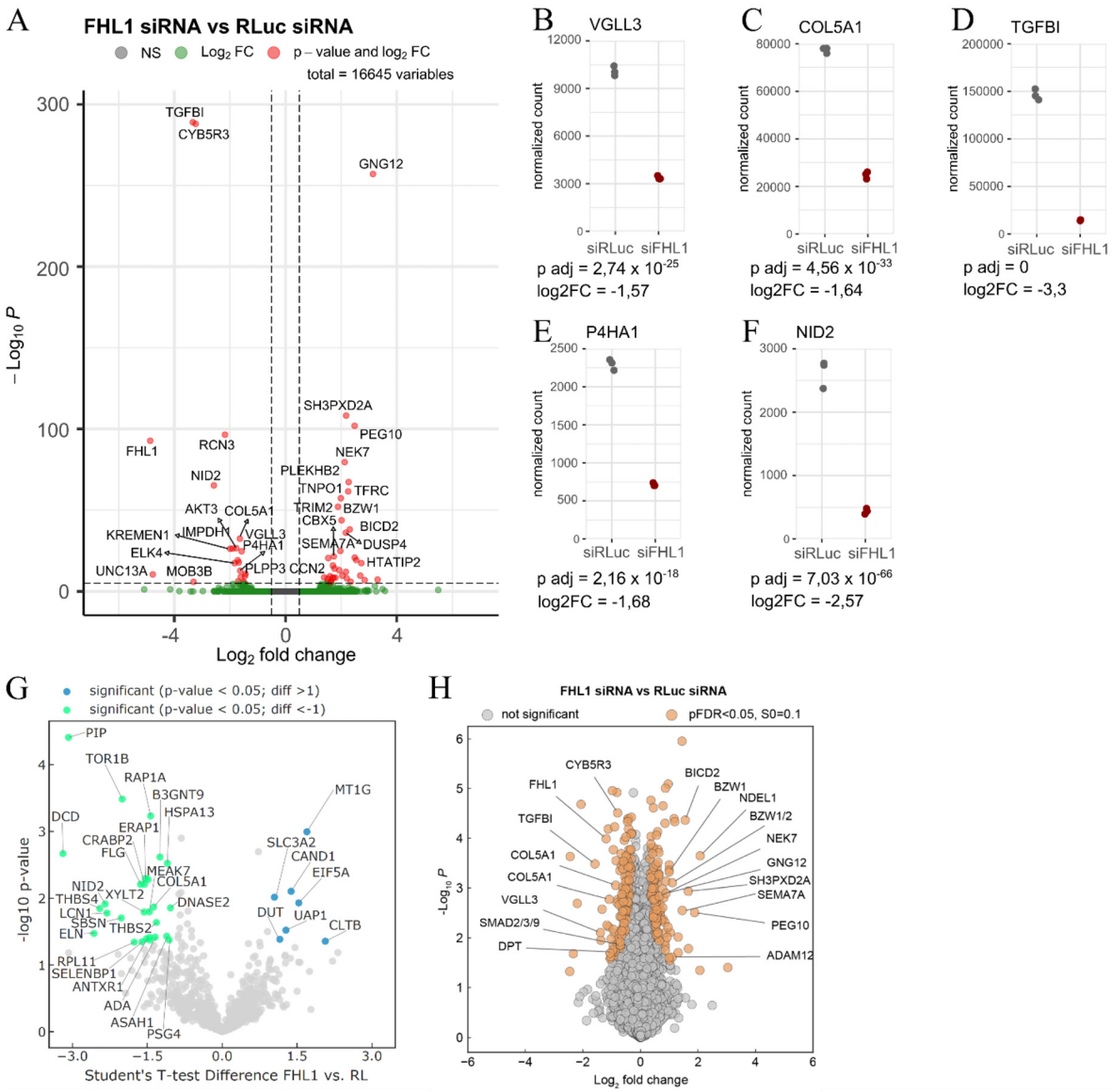

Figure 6. Omics data of *FHL1* siRNA (siFHL1) and *RLuc* siRNA (siRLuc) treated primary fibroblasts and their supernatants. (A) Volcano plot of bulk RNA-seq data, depicting the most upregulated and downregulated genes in siFHL1-treated samples compared to siRLuc-treated. Grey dots: nonsignificant (NS) genes; green dots: genes with a significant Log2FC; red dots: genes with a significant *P* adjusted and Log2FC value. Log2FC smaller than −0.5 or larger than 0.5 and *P* adjusted value <.05 were considered significant, cutoffs are displayed by a dotted line. (B) *VGLL3*, (C) *COL5A1*, (D) *TGFBI*, (E) *P4HA1*, and (F) *NID2* expression in siRLuc- and siFHL1-treated fibroblasts from the bulk RNA-seq data. Transcriptomics: N = 3/3 independent samples. (G) Volcano plot showing the log2 fold change and -log10 *P* value of secreted proteins after treatment with siFHL1 compared to siRLuc (RL). Significantly enriched proteins were determined by an unpaired 2-sided Student's *t*-test. (H) Volcano plot depicting the log2 fold change and −log10 *P* value of proteins in the cell lysate following downregulation of *FHL1* compared to siRLuc-treated samples. Orange: significantly regulated proteins. Significance determined by paired Welch's t-test with permutation-based FDR <0.05 and S0 = 0.1. Secretomics and proteomics: N = 5/5 independent samples. COL5A1, collagen V α1 chain; FHL1, four and a half LIM domain 1; NID2, nidogen 2; P4HA1, prolyl 4-hydroxylase subunit alpha 1; SSc, systemic sclerosis; TGFBI, transforming growth factor beta-induced protein; VGLL3, vestigial-like family member 3; FDR, False Discovery Rate.

hydroxylase subunit alpha 1 (*P4HA1*) (Fig 6A-F). Gene ontology (GO) term analysis for downregulated genes included chaperone-mediated protein folding and metabolic processes, yet a more significant correlation was seen for the terms extracellular structure organisation, ECM organisation, and external encapsulating structure organisation, while the upregulated GO terms were closely linked to proliferation and mitosis (Supplementary Fig S4C).

Focusing on genes involved in ECM homeostasis or its regulation, *VGLL3* stood out. It acts as a transcription cofactor for TEA (Transcriptional Enhancer Factor-1 DNA-binding domain) domain-containing transcription factors and is known to promote collagen expression and production in myofibroblasts and to be induced by matrix stiffness, creating a positive feedback loop for collagen production by myofibroblasts [16]. Our data revealed that knockdown of *FHL1* significantly reduced *VGLL3* expression (Fig 6B).

Secretomics analysis of supernatants from *FHL1* siRNA-treated cells supported the gene expression pattern examined in the transcriptome analysis following *FHL1* downregulation (Fig 6G). Notably, extracellular proteins COL5A1, NID2, and elastin (ELN) were significantly less abundant in the culture supernatants (Fig 6G).

Also, proteomics analysis of the cell layer from *FHL1* siRNA-treated fibroblasts not only demonstrated a ~50% downregulation of FHL1 protein, but further corroborated the significant downregulation of TGFBI and COL5A1 as well as the significant

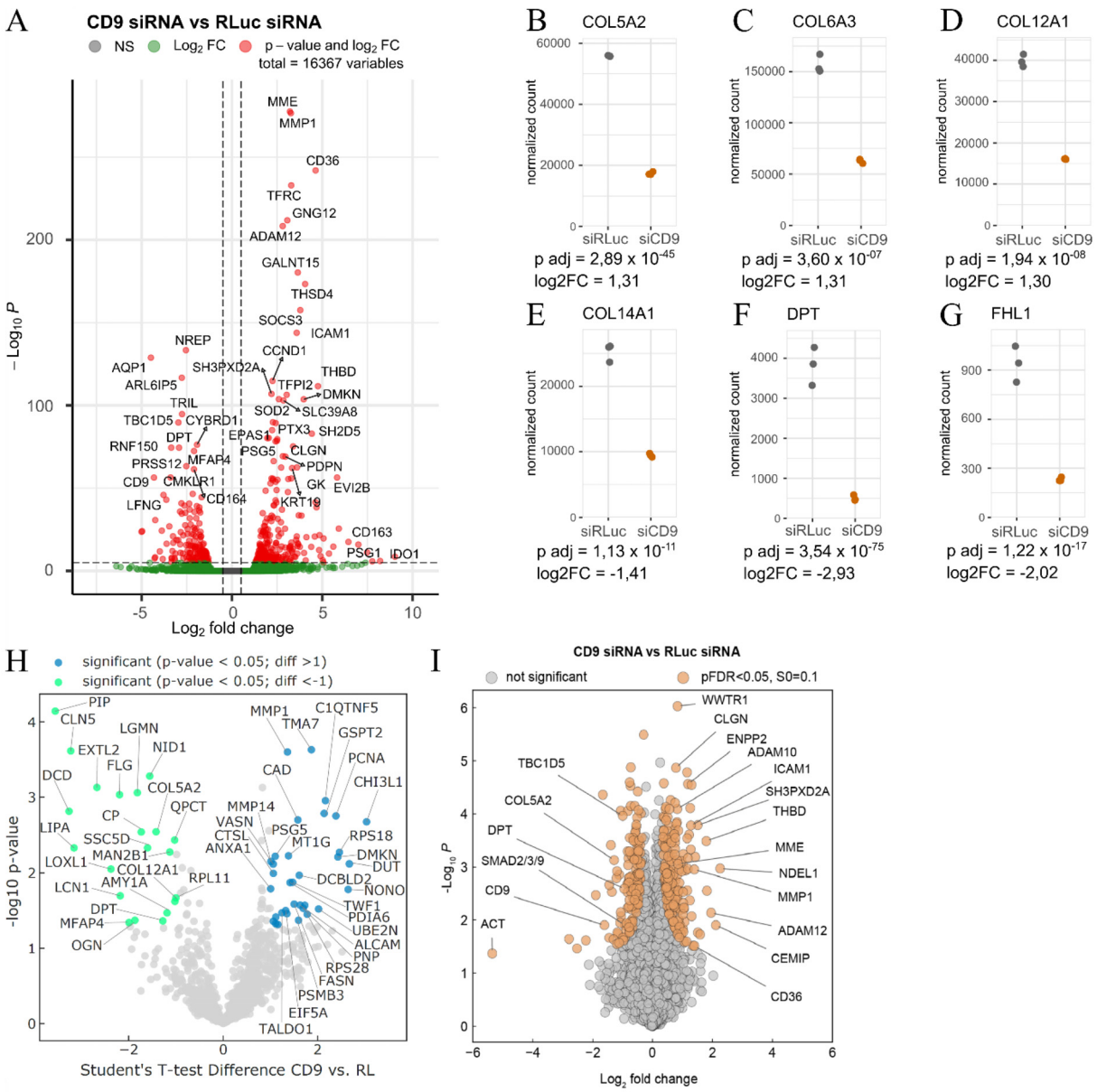

Figure 7. Omics data from *CD9* siRNA (siCD9) and siRLuc-treated primary dermal fibroblasts. (A) Volcano plot from bulk transcriptomics data showing the most upregulated and downregulated genes in siCD9-treated samples compared to siRLuc-treated. Grey dots: nonsignificant (NS) genes; green dots: genes with a significant Log2FC; red dots: genes with a significant *P* adjusted and Log2FC value. Log2FC less than −0.5 or larger than 0.5 and *P* adjusted value <.05 were considered significant, cutoffs depicted with a dotted line. Transcriptomics data of (B) *COL5A2*, (C) *COL6A3*, (D) *COL12A1*, (E) *COL14A1*, (F) *DPT*, and (G) *FHL1* expression in siRLuc- and siCD9-treated fibroblasts. Transcriptomics: N = 3/3 independent samples. (H) Volcano plot showing the log2 fold change and −log10 *P* value of secreted proteins after treatment with siCD9 compared to siRLuc. Significantly enriched proteins were determined by a 2-sided Student's *t*-test. (I) Volcano plot depicting proteomic changes upon downregulation of *CD9* compared to siRLuc-treated samples. Orange: significantly regulated proteins. Significance determined by Welch's t-test with permutation-based FDR <0.05 and S0 = 0.1. Secretomics and proteomics: N = 5/5 independent samples. COL5A2, collagen V α2 chain; COL6A3, Collagen 6 α3 chain; COL12A1, Collagen 12 α1 chain; COL14A1, Collagen 14 α1 chain; DPT, dermatopontin; FHL1, four and a half LIM domain 1; SSc, systemic sclerosis; FDR, False Discovery Rate.

upregulation of SH3 And PX Domains 2A (SH3PXD2A) and NIMA-Related Kinase 7 (NEK7). Notably, *FHL1* siRNA treatment significantly downregulated VGLL3, SMAD2, and SMAD3, which are both key to TGF-beta signalling [30], as well as SMAD9 (Fig 6H), linked to BMP signalling [31].

Similarly, we saw significant differences in the gene expression profiles when comparing *CD9* siRNA and *RLuc* siRNA-treated samples (Supplementary Fig S5A), showing significant CD9 downregulation (−4.32 log2FC; Supplementary Fig S5B). Fibroblasts treated with *CD9* siRNA revealed a significant downregulation of genes such as neuronal regeneration related protein (*NREP*), aquaporin 1 (*AQP1*), *ARL6IP5* (Adenosine diphosphate (ADP)−ribosylation factor−like GTPase 6 −interacting protein 5), dermatopontin (*DPT*), and microfibril associated protein 4 (*MFAP4*); and a significant upregulation of genes such as membrane metalloendopeptidase (*MME*), matrix metallopeptidase 1 (*MMP1*), ADAM metallopeptidase domain 12 (*ADAM12*), and thrombospondin type 1 domain containing 4 (*THSD4*) (Fig 7A). In addition, GO-term enrichment analysis identified that upregulated genes were mainly involved in DNA replication and mitosis checkpoint signalling (Supplementary Fig S5C). In contrast, the downregulated genes were associated with cytoplasmic translation, negative regulation of endothelial cell migration and phospholipase C-activating G protein-coupled receptor signalling (Supplementary Fig S5C). Notably, we also identified a number of genes involved in ECM production or its

regulation, including a significant downregulation of collagens *COL5A2*, *COL6A3*, *COL12A1*, *COL14A1*, and *COL21A1* (Fig 7B-E, Supplementary Fig S5D). In addition, *IGFBP5* (Supplementary Fig S5E), *DPT*, and most interestingly *FHL1* were downregulated (Fig 7F,G).

To functionally link CD9 expression with regulation of ECM deposition, fibroblasts from *CD9*$^{-/-}$ mouse embryonic fibroblasts (*CD9* KO MEFs) and control MEFs were analysed by bulk RNA sequencing (Supplementary Fig S6A-C). Several major collagens and *Acta2* (α-SMA) were significantly downregulated in the *CD9* KO MEFs, also at the protein level (Supplementary Fig S6C-I, Supplementary Fig S7A-E).

Findings based on *CD9* knockout MEFs were further corroborated by *CD9* gene silencing in human skin fibroblasts. Secretomic analysis of supernatants from *CD9* siRNA and *RLuc* siRNA-treated human primary fibroblasts revealed similar changes at the protein level. Secreted extracellular proteins COL5A2, COL12A1, and DPT were significantly reduced in the *CD9* siRNA-treated samples (Fig 7H). In addition, MFAP4, an ECM protein regulating elastic fibre assembly [32], Lysyl oxidase like 1 (LOXL1), which crosslinks elastin and collagens and has been associated with fibrosis [33], and osteoglycin (OGN), which is involved in the organisation and maintenance of ECM and was described as a key regulator of fibrosis, were all significantly decreased following *CD9* knockdown (Fig 7H).

In addition, proteomics analysis of cell lysates from *CD9* siRNA-treated fibroblasts supports the transcriptomics analysis and the biological relevance of CD9. This was further underscored by a decrease of TGF-beta signalling associated SMAD2 and SMAD3 as well as SMAD9 in response to *CD9* knockdown (Fig 7I).

VGLL3 is significantly upregulated in subsets of SSc dermal fibroblasts and SSc skin

Downregulation of *FHL1* by siRNA demonstrated that VGLL3 expression was markedly reduced. Because VGLL3 is known to play an important role in promoting ECM expression, we also analysed its expression in the different clusters representing fibroblast subpopulations. Although our scRNA-seq data indicated no significant difference in the overall *VGLL3* expression between SSc and healthy control fibroblasts, we observed the highest expression levels of *VGLL3* overall in cluster 3 (IGFBP4^{hi}), which also had high expression levels of both *FHL1* and *CD9* (Fig 8A,B; Fig 2B,C). In addition, clusters 1 (DCN^{hi}) and 10 (FHL1^{hi}) also displayed increased expression levels of *VGLL3*, yet to a lesser extent than cluster 3 (IGFBP4^{hi}) (Fig 8A,B).

Of note, the number of *FHL1*$^{+}$/*VGLL3*$^{+}$ double-positive fibroblasts in our scRNA-seq data was significantly increased in SSc when compared to healthy control fibroblasts: 243 control compared to 2197 SSc fibroblasts with high expression of both, *FHL1* and *VGLL3* (expression level >1.2), equivalent to 1.27% of control and 12.01% of SSc fibroblasts (Supplementary Fig S8A, B). Cells coexpressing *VGLL3* and *FHL1* mainly localised to cluster 1 (DCN^{hi}) in control fibroblasts and to an even higher extent to cluster 3 (IGFBP4^{hi}) in SSc fibroblasts (Fig 8C).

Likewise, the abundance of *CD9*$^{+}$/*VGLL3*$^{+}$ double-positive fibroblasts was also significantly augmented in SSc compared to healthy control fibroblasts: 225 control vs 787 SSc fibroblasts with high expression of both, *CD9* and *VGLL3* (expression level >1.2), equating to 1.17% of control and 4.30% of SSc fibroblasts (Supplementary Fig S8C,D). *CD9*$^{+}$/*VGLL3*$^{+}$ fibroblasts mainly localised to cluster 3 (IGFBP4^{hi}) in SSc fibroblasts, as did the *FHL1*$^{+}$/*VGLL3*$^{+}$ fibroblasts (Supplementary Fig S8E).

Strikingly, we also identified fibroblasts that coexpressed all 3 genes (*CD9*, *FHL1*, and *VGLL3*) with high intensity (expression level >1.2). Their abundance was significantly increased in SSc compared to controls: we identified 393 *CD9*$^{+}$/*FHL1*$^{+}$/*VGLL3*$^{+}$ fibroblasts in SSc, but only 4 such fibroblasts in controls, which was equivalent to 2.14% of the SSc vs 0.02% of the control fibroblast population (Supplementary Fig S8F,G). Given that *CD9*$^{+}$/*FHL1*$^{+}$/*VGLL3*$^{+}$ fibroblasts were predominantly found in SSc samples, they may represent a specific subtype of fibroblasts present in SSc. Importantly, IF staining confirmed increased VGLL3 expression in SSc fibroblast cultures and in addition in patient biopsies (Fig 8D-F) indicating potential diagnostic and therapeutic implications.

DISCUSSION

SSc (scleroderma; SSc) is an autoimmune-driven disease, where an initial inflammatory reaction leads to activation of fibroblasts and excessive deposition of ECM [1,2,34]. Fibroblasts cultured from skin biopsies obtained from patients with SSc show induced collagen synthesis even after several passages [11–13]. We here provide evidence by scRNA-seq that fibroblast cultures obtained by outgrowth from skin biopsies from fibrotic skin of patients with dcSSc are composed of a heterogenous group of fibroblasts and represent an important source to identify altered fibroblast subsets with a stable phenotype independent of the environment. In these, we demonstrate upregulation of novel genes characteristic of SSc fibroblast clusters and propose that they have a functional role in ECM deposition.

Extensive scRNA-seq data from fibroblasts isolated directly from the skin of patient with SSc also characterised distinct fibroblast subsets [9,35–38]. This experimental approach has the advantage of better reflecting the state of activity of cells in their biological environment. On the other hand, the sensitivity of certain fibroblasts to enzymatic digestion may result in the selection of more resistant populations. Comparison of this kind of scRNA-seq data with our fibroblast populations revealed only limited similarities and did not detect several clusters reported previously [8,9]. This can be due to the culture conditions modifying the gene expression profile to a certain extent. Another contributing difference may be that the heterogeneity of fibroblasts detected directly after isolation from the tissue might only reflect a transient dynamic state of the cells at a distinct point in time and not the presence of stable fibroblast populations. In contrast, our cultured fibroblasts were analysed after 4 passages and revealed a relatively stable phenotype.

Our data indicate that the fibroblasts obtained from the patients with SSc did not reveal a clear papillary or reticular gene signature. We identified the papillary marker gene, *DPP4*, in all fibroblasts, but simultaneously also the expression of the reticular marker gene, *ATXN1*. However, in cluster 1 (DCN^{hi}) and interestingly in cluster 3 (IGFBP5^{hi}), we saw *PDPN* expression, characteristic for reticular fibroblasts that are derived from deep dermal tissue, where most of the fibrotic activity in SSc takes place. Furthermore, several of the subsets in our scleroderma cultures did exhibit markers of activation that were previously identified by several other groups [3,39].

FHL1 and CD9 overexpressing fibroblasts in SSc and in fibrotic murine skin

Of note, we report the detection of unique populations characterised by high overexpression of CD9 and FHL1. This raised the question whether these populations represent activated

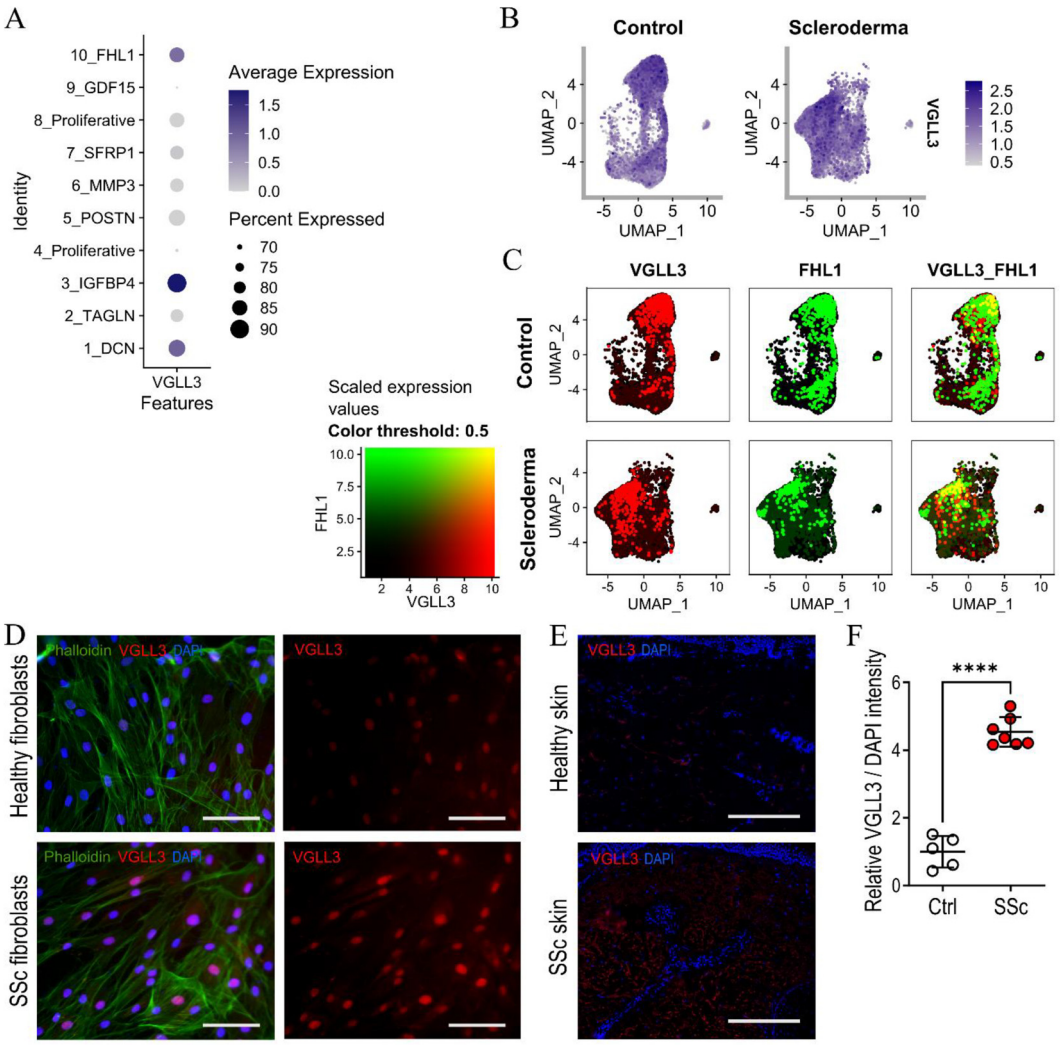

Figure 8. VGLL3 expression is increased in specific subsets of fibroblasts obtained from patients with dcSSc. (A) scRNA-seq dot plot of *VGLL3*. The size of the dot is proportional to the percentage of cells per cluster expressing the gene. The colour intensity correlates with the scaled average expression intensity in these cells. (B) scRNA-seq feature plots of *VGLL3* for control (left) and dcSSc (right) fibroblasts. Each dot represents a cell; the darker the colour intensity of the dots, the more increased the gene expression. (C) Coexpression feature plot of *VGLL3* and *FHL1* comparing healthy control (top row) and dcSSc (bottom row) fibroblasts. Red dots represent the expression of *VGLL3*, green dots the expression of *FHL1*; high coexpression of *VGLL3* and *FHL1* can be seen as yellow. Each dot represents a cell, and the increased intensity of the colour of the dots represents increased expression. The colour scale (on the left) depicts increased coexpression in a cell with a yellow to orange colour scale. (D) Representative IF staining of DAPI (blue), phalloidin (green), and VGLL3 (red) in human healthy (top row) and dcSSc fibroblasts (bottom row). Scale bar = 100 μm. (E) IF staining of DAPI (blue) and VGLL3 (red) in human healthy skin (top) and skin from patients with dcSSc (bottom). Scale bar = 300 μm. (F) Quantification of IF staining intensity of VGLL3 normalised to DAPI in human healthy and SSc dermis. Data are shown as relative values compared to control (N = 4 Ctrl/7 SSc donors; **** $P \leq .0001$). *P* values calculated with Welch's t-test, two-tailed; data shown as mean ± SD. Ctrl, control; dcSSc, diffuse cutaneous systemic sclerosis; FHL1, four and a half LIM domain 1; IF, immunofluorescent; scRNA-seq, single-cell RNA sequencing; SSc, systemic sclerosis; VGLL3, vestigial-like family member 3; UMAP, Uniform Manifold Approximation and Projection; DAPI, 4',6-diamidino-2-phenylindole.

fibroblasts. Given the expression of several markers for activated fibroblasts in these subpopulations, such as the profibrotic markers *THY1* (CD90), *CTGF*, *TNC*, *IGFBP5*, *ACTA2*, among others, we think they do. Expression of *ACTA2*, in particular, has been described as a characteristic marker of myofibroblasts [40,41], which play a key role in tissue repair and fibrotic diseases [42].

However, we also identified clusters characterised by *FHL1* and *CD9* overexpression, where *ACTA2* was not overexpressed. Also, *CD9* overexpression was found to be associated only partially with *FHL1* co-overexpression. This indicates further heterogeneity within the still insufficiently characterised myofibroblasts [9] and suggests the presence of at least 3 related but distinct subpopulations of $CD9^+$, $CD9^+/FHL1^+$, and $FHL1^+$ cells, with presumably specific functions.

FHL1 has been shown to play an essential role in muscle development and related diseases. It is also reported to be downregulated in cancer. There are studies indicating that the isoform FHL1A is expressed in skeletal muscle, myocardium and in fibroblasts [14,26]. To date, its role in the biology of fibroblasts is unknown and it has not previously been described in the context of fibrotic diseases.

CD9 is a tetraspanin transmembrane protein and is thought to mark exosomes. It is associated with many cellular functions in various cell types and interacts with integrins and other cell surface molecules that are involved in cell–matrix interactions. It has been linked to multiple diseases associated with dysregulated inflammatory responses and various types of cancer [15]. Mice lacking *CD9* have severe fertility issues [43], and exhibit delayed wound healing [44]. In addition, CD9 levels were reported to be

increased in SSc dermal fibroblasts [39]. However, due to the broad cellular distribution of CD9, a causal relationship with the fibrotic process and its role in fibroblasts is still speculative.

Our western blots and proteomics analysis comparing patients with SSc-derived cultured fibroblasts with healthy controls further corroborated the increased levels for CD9 and FHL1 that we detected by scRNA-seq and confirmed previous findings by Nakamura et al [39] for CD9. Moreover, we also detected the FHL1 and CD9 overexpressing subpopulations *in vivo* in biopsies from patients with SSc by immunofluorescence. Together, these findings argue strongly against a culture condition-dependent artefact and indicate that these subpopulations represent a stable subset of activated fibroblasts in SSc.

Immunostaining of biopsies obtained from severe fibrotic skin from patients with dcSSc revealed that FHL1 staining was most prominent in spindle-shaped cells with the histological appearance of fibroblasts in the reticular layer of the dermis. Interestingly, CD9 was also overexpressed in keratinocytes in these biopsies compared to controls. Keratinocyte involvement in the pathophysiology of scleroderma has recently been discussed, but it remains to be clarified, whether this is directly related to the disease or represents a secondary phenomenon [45–47].

We also found that fibroblasts obtained from patients with lcSSc did not overexpress FHL1 to the same extent as fibroblasts from patients with dcSSc. Also, FHL1 and CD9 staining in biopsies from patients with lcSSc were similar to controls or showed only a slight increase. Since the development of fibrosis was much more intense in the patients with dcSSc, this indicates that induced FHL1 and CD9 expression are characteristic of heavily involved fibrotic skin and reflects the intensity of fibrosis. This might indicate that the expression of these markers in distinct fibroblast subsets can be used as biomarkers for following the severity of fibrosis.

The association of CD9 and FHL1 overexpressing fibroblasts with the initiation of a fibrotic reaction is further supported by the demonstration of increased numbers of CD9 and FHL1 strongly positive fibroblasts in the bleomycin-induced fibrotic skin in mice.

FHL1 and CD9 have a functional role in activated fibroblast subpopulations

Evidently, the elevated expression levels and also the induced protein levels in culture and *in vivo* represent a descriptive analysis and do not allow a causal connection between CD9/FHL1 and the activation of fibroblast subsets. Knockdown experiments were therefore conducted to reveal if FHL1 and CD9 have functional roles in the activation of these fibroblast subsets. The functional analysis of *CD9* downregulation in human fibroblasts revealed reduced expression of genes involved in cytoplasmic protein translation, but also of *MFAP4*, dermatopontin, several collagens, and other ECM-related genes. In addition, we obtained independent evidence for a functional role of CD9 from another system. Analysis of murine *CD9* KO MEFs by RNA-seq revealed a very significant downregulation of both *Col1a1* and *Col1a2* along with other collagens. Interestingly, *Acta2* was also significantly downregulated in these murine fibroblasts. Notably, collagen I, fibrillin 1, and fibronectin were also downregulated in the *CD9* KO MEFs at the protein level. We were able to confirm that a lack of CD9 has a negative impact on ECM-related genes and proteins in several different cross-species assays.

Similarly, downregulation of *FHL1* resulted in reduced expression of TGFBI, known to be involved in the organisation of the ECM [48], as well as of several genes encoding ECM or ECM-modifying enzymes. Moreover, both *FHL1* and *CD9* downregulation by siRNA treatment resulted in downregulation of SMAD2 and SMAD3 proteins, as targets in the TGF-β signalling pathways, indicating a direct impact on ECM gene transcription.

Interestingly, also the transcription cofactor VGLL3 was downregulated after FHL1 knockdown. VGLL3 was previously reported to be involved in regulating the induction of collagen synthesis in myofibroblasts in response to mechanical stress [16], and it is also involved in myogenesis, cell proliferation [49], and autoimmune diseases [50]. Altered interaction of fibroblasts with the surrounding ECM in a very stiff tissue is thought to play a key role in the persistent activation of fibroblasts during fibrosis. VGLL3 was recently reported to be translocated to the nucleus in response to substrate stiffness and to induce collagen production by suppressing miR-29b, which is known to target collagen mRNA [16]. Our data demonstrated an upregulation of VGLL3 in SSc-derived dermal fibroblasts in culture and also in SSc skin sections of the fibrotic tissue. This strongly supports a role of VGLL3 in fibrosis and provides a molecular explanation for the perpetuation of an activated phenotype of the myofibroblast subsets in SSc due to the increased mechanical stiffness of the tissue, which is mediated through the integrin-cytoskeleton axis [51–53].

Downregulation of *FHL1* resulted in the regulation of several other ECM genes, eg, collagen V (COL5A1), NID2, *P4HA1*, and ELN. The decrease in COL5A1 and NID2 was confirmed by proteomic analysis of secreted proteins. This altered expression of distinct molecules that are involved in the collagen suprastructure and macromolecular association is in accordance with the disturbed structure of collagen bundles seen in biopsies from patients with SSc by electron microscopy [54]. The subsequently altered macromolecular ECM organisation is thought to contribute to the increased stiffness of the tissue, which again leads to activation of certain fibroblast subsets and contributes to the perpetuation of the activation.

Strikingly, *CD9* downmodulation by siRNA resulted in reduced *FHL1* transcript levels, as well as other ECM-related genes, such as collagen V (*COL5A2*), *DPT*, and *MFAP4*. Other ECM-related proteins were also impacted, including LOXL1 and collagen XII (COL12A1). The downregulation of *FHL1* after *CD9* knockdown indicates a close link between these proteins in the differently activated subsets of (myo)fibroblasts. It still remains unclear if a hierarchical process exists placing CD9 upstream of FHL1 that results in VGLL3 induction, whether shared upstream pathways exist or whether these players act independently. Nevertheless, the induction of VGLL3 is in line with the activation of collagen synthesis in the fibroblast populations reported here and demonstrated in a recent report on its role in cardiac fibrosis [16].

Conclusion

We identify a novel subset of fibroblasts characterised by high expression of CD9 and FHL1 in fibrotic lesions of patients with dcSSc and present evidence in different experimental systems supporting a functional role of these proteins for ECM production and fibrosis development. The data provide the basis for new biomarker development and the identification of novel therapeutic targets.

Competing interests

The authors have declared that no conflict of interest exists.

CRediT authorship contribution statement

Ann-Helen S Rosendahl: Writing – review & editing, Writing – original draft, Visualization, Methodology, Investigation, Conceptualization. **Anna Bornikoel:** Writing – review & editing, Writing – original draft, Visualization, Methodology, Investigation. **Isabel Zeinert:** Writing – review & editing, Methodology. **Lena Keufgens:** Writing – review & editing, Visualization, Methodology. **Frederik Tellkamp:** Writing – review & editing, Visualization, Methodology. **Niklas Kleinenkuhnen:** Writing – review & editing, Methodology. **Till Baar:** Writing – review & editing, Methodology, Investigation. **Katrin Schönborn:** Writing – review & editing, Visualization, Funding acquisition. **Marcus Krüger:** Writing – review & editing, Supervision. **Achim Tresch:** Writing – review & editing, Supervision. **Bent Brachvogel:** Writing – review & editing, Methodology, Funding acquisition, Conceptualization. **Beate Eckes:** Writing – review & editing, Project administration, Funding acquisition, Conceptualization. **Pia Moinzadeh:** Writing – review & editing, Investigation. **Thomas Krieg:** Writing – review & editing, Writing – original draft, Supervision, Project administration, Funding acquisition, Conceptualization.

Acknowledgements

We thank Dr Claude Boucheix, Dr Eric Rubinstein, and Dr Stephanie Charrin (INSERM, Paris, France) for the kind gift of *CD9* KO and control MEFs, Dr Miloš Gojković (CECAD Cologne) for help and expert advice with the fluorescence-activated cell sorting data, and Susanne Neumann for excellent technical assistance. Some of the data reported here were presented at ISID2023 conference in Tokyo (DOI:10.1016/j.jid.2023.03.1472), and at the ESDR 2022 conference in Amsterdam (DOI:10.1016/j.jid.2022.09.018).

Funding

A-HSR was generously supported by the Young researcher grant, year 2021 from Emil Aaltonen Foundation, Finland. Parts of this work were funded by CMMC (SRG 2), CECAD (both to TK), Edith Busch Foundation (to BE and KS) and the German Research Foundation through KR 558/17-1, project ID 468236352 (to TK) and RU 2722, project ID 384170921 (to BB). CECAD/ZMMK Proteomics Facility appreciates the funding of DFG Grossgeräteantrag 'INST 216/1020-1 FUGG'.

Patient consent for publication

Written informed consent was obtained from the patients.

Ethics approval

This study has the approval of the local ethics committee (Ethics committee of the medical faculty of University of Cologne, 21-1072). The study was conducted in accordance with the criteria set by the Declaration of Helsinki. Mouse handling and experimentation were performed according to the German Law for Welfare of Laboratory Animals and were approved by the North Rhine Westphalia State Office for Nature, Environment and Consumer Protection Germany (LANUV NRW) under the license 84-02.04.2020.A155.

Provenance and peer review

Not commissioned; externally peer reviewed.

Supplementary materials

Supplementary material associated with this article can be found, in the online version, at doi:10.1016/j.ard.2025.11.027.

Orcid

Ann-Helen S Rosendahl: http://orcid.org/0000-0001-7968-0990
Anna Bornikoel: http://orcid.org/0000-0002-1921-7205
Thomas Krieg: http://orcid.org/0000-0001-5616-8476

REFERENCES

[1] Gabrielli A, Avvedimento EV, Scleroderma Krieg T. N Engl J Med 2009;360(19):1989–2003.
[2] Varga J, Abraham D. Systemic sclerosis: a prototypic multisystem fibrotic disorder. J Clin Invest 2007;117(3):557–67.
[3] Driskell RR, Lichtenberger BM, Hoste E, Kretzschmar K, Simons BD, Charalambous M, et al. Distinct fibroblast lineages determine dermal architecture in skin development and repair. Nature 2013;504(7479):277–81.
[4] Driskell RR, Watt FM. Understanding fibroblast heterogeneity in the skin. Trends Cell Biol 2015;25(2):92–9.
[5] Philippeos C, Telerman SB, Oulès B, Pisco AO, Shaw TJ, Elgueta R, et al. Spatial and single-cell transcriptional profiling identifies functionally distinct human dermal fibroblast subpopulations. J Invest Dermatol 2018;138(4):811–25.
[6] Sawant M, Hinz B, Schönborn K, Zeinert I, Eckes B, Krieg T, et al. A story of fibers and stress: matrix-embedded signals for fibroblast activation in the skin. Wound Repair Regen 2021;29(4):515–30.
[7] Koliaraki V, Prados A, Armaka M, Kollias G. The mesenchymal context in inflammation, immunity and cancer. Nat Immunol 2020;21(9):974–82.
[8] Tabib T, Morse C, Wang T, Chen W, Lafyatis R. SFRP2/DPP4 and FMO1/LSP1 define major fibroblast populations in human skin. J Invest Dermatol 2018;138(4):802–10.
[9] Tabib T, Huang M, Morse N, Papazoglou A, Behera R, Jia M, et al. Myofibroblast transcriptome indicates $SFRP2^{hi}$ fibroblast progenitors in systemic sclerosis skin. Nat Commun 2021;12(1):4384.
[10] Valenzi E, Bulik M, Tabib T, Morse C, Sembrat J, Trejo Bittar H, et al. Single-cell analysis reveals fibroblast heterogeneity and myofibroblasts in systemic sclerosis-associated interstitial lung disease. Ann Rheum Dis 2019;78(10):1379–87.
[11] LeRoy EC. Increased collagen synthesis by scleroderma skin fibroblasts in vitro: a possible defect in the regulation or activation of the scleroderma fibroblast. J Clin Invest 1974;54(4):880–9.
[12] LeRoy EC, Mercurio S, Sherer GK. Replication and phenotypic expression of control and scleroderma human fibroblasts: responses to growth factors. Proc Natl Acad Sci U S A. 1982;79(4):1286–90.
[13] Fleischmajer R, Perlish JS, Krieg T, Timpl R. Variability in collagen and fibronectin synthesis by scleroderma fibroblasts in primary culture. J Invest Dermatol 1981;76(5):400–3.
[14] Shathasivam T, Kislinger T, Gramolini AO. Genes, proteins and complexes: the multifaceted nature of FHL family proteins in diverse tissues. J Cell Mol Med 2010;14(12):2702–20.
[15] Brosseau C, Colas L, Magnan A, Brouard S. CD9 Tetraspanin: a new pathway for the regulation of inflammation? Front Immunol 2018;9:2316.
[16] Horii Y, Matsuda S, Toyota C, Morinaga T, Nakaya T, Tsuchiya S, et al. VGLL3 is a mechanosensitive protein that promotes cardiac fibrosis through liquid-liquid phase separation. Nat Commun 2023;14(1):550.
[17] Satija R, Farrell JA, Gennert D, Schier AF, Regev A. Spatial reconstruction of single-cell gene expression data. Nat Biotechnol 2015;33(5):495–502.
[18] McGinnis CS, Murrow LM, Gartner ZJ. DoubletFinder: doublet detection in single-cell RNA sequencing data using artificial nearest neighbors. Cell Syst 2019;8(4):329–37 .e4.
[19] Stuart T, Butler A, Hoffman P, Hafemeister C, Papalexi E, Mauck 3rd WM, et al. Comprehensive integration of single-cell data. Cell 2019;177(7):1888–902 .e21.
[20] Sawant M, Wang F, Koester J, Niehoff A, Nava MM, Lundgren-Akerlund E, et al. Ablation of integrin-mediated cell-collagen communication alleviates fibrosis. Ann Rheum Dis 2023;82(11):1474–86.

[21] Nolte H, MacVicar TD, Tellkamp F, Krüger M. Instant clue: a software suite for interactive data visualization and analysis. Sci Rep 2018;8(1):12648.
[22] Demichev V, Messner CB, Vernardis SI, Lilley KS, Ralser M. DIA-NN: neural networks and interference correction enable deep proteome coverage in high throughput. Nat Methods 2020;17(1):41–4.
[23] Tusher VG, Tibshirani R, Chu G. Significance analysis of microarrays applied to the ionizing radiation response. Proc Natl Acad Sci U S A 2001;98(9):5116–21.
[24] LeRoy EC, Medsger TA. Jr. Criteria for the classification of early systemic sclerosis. J Rheumatol 2001;28(7):1573–6.
[25] Selva-O'Callaghan A, Trallero-Araguás E, MT Sanz-Martínez. Anti-FHL1 antibody: welcome to a novel autoantibody in myositis. Rheumatology (Oxford) 2022;61(10):3887–8.
[26] Tao Y, Wu Y, Shen R, He S, Miao X. Role of four and a half LIM domain protein 1 in tumors (Review). Oncol Lett 2025;29(1):37.
[27] Yang K, Huang N, Sun J, Dai W, Chen M, Zeng J. Transforming growth factor-beta induced protein regulates pulmonary fibrosis via the G-protein signaling modulator 2 /Snail axis. Peptides 2022;155:170842.
[28] Wu M, Wang Z, Shi X, Zan D, Chen H, Yang S, et al. TGFβ1-RCN3-TGFBR1 loop facilitates pulmonary fibrosis by orchestrating fibroblast activation. Respir Res 2023;24(1):222.
[29] Sun M, Chen S, Adams SM, Florer JB, Liu H, Kao WW, et al. Collagen V is a dominant regulator of collagen fibrillogenesis: dysfunctional regulation of structure and function in a corneal-stroma-specific Col5a1-null mouse model. J Cell Sci 2011;124(Pt 23):4096–105.
[30] Peng D, Fu M, Wang M, Wei Y, Wei X. Targeting TGF-beta signal transduction for fibrosis and cancer therapy. Mol Cancer 2022;21(1):104.
[31] Tsukamoto S, Mizuta T, Fujimoto M, Ohte S, Osawa K, Miyamoto A, et al. Smad9 is a new type of transcriptional regulator in bone morphogenetic protein signaling. Sci Rep 2014;4:7596.
[32] Mohammadi A, Sorensen GL, Pilecki B. MFAP4-Mediated effects in elastic fiber homeostasis, integrin signaling and cancer, and its role in teleost fish. Cells 2022;11(13):2115.
[33] Greene AG, Eivers SB, Dervan EWJ, O'Brien CJ, Wallace DM. Lysyl oxidase like 1: biological roles and regulation. Exp Eye Res 2020;193:107975.
[34] Distler JHW, Györfi AH, Ramanujam M, Whitfield ML, Königshoff M, Lafyatis R. Shared and distinct mechanisms of fibrosis. Nat Rev Rheumatol 2019;15 (12):705–30.
[35] Werner G, Sanyal A, Mirizio E, Hutchins T, Tabib T, Lafyatis R, et al. Single-cell transcriptome analysis identifies subclusters with inflammatory fibroblast responses in localized scleroderma. Int J Mol Sci 2023;24(12):9796.
[36] Li Z, Cao T, Li Q, Zhang J, Du J, Chen J, et al. Cross-disease characterization of fibroblast heterogeneities and their pathogenic roles in skin inflammation. Clin Immunol 2023;255:109742.
[37] Clark KEN, Xu S, Attah M, Ong VH, Buckley CD, Denton CP. Single-cell analysis reveals key differences between early-stage and late-stage systemic sclerosis skin across autoantibody subgroups. Ann Rheum Dis 2023;82(12):1568–79.
[38] Zhu H, Luo H, Skaug B, Tabib T, Li YN, Tao Y, et al. Fibroblast subpopulations in systemic sclerosis: functional implications of individual subpopulations and correlations with clinical features. J Invest Dermatol 2024;144(6):1251–61 .e13.
[39] Nakamura K, Jinnin M, Harada M, Kudo H, Nakayama W, Inoue K, et al. Altered expression of CD63 and exosomes in scleroderma dermal fibroblasts. J Dermatol Sci 2016;84(1):30–9.
[40] Majno G, Gabbiani G, Hirschel BJ, Ryan GB, Statkov PR. Contraction of granulation tissue in vitro: similarity to smooth muscle. Science 1971;173 (3996):548–50.
[41] Hirschel BJ, Gabbiani G, Ryan GB, Majno G. Fibroblasts of granulation tissue: immunofluorescent staining with antismooth muscle serum. Proc Soc Exp Biol Med 1971;138(2):466–9.
[42] Hinz B, Lagares D. Evasion of apoptosis by myofibroblasts: a hallmark of fibrotic diseases. Nat Rev Rheumatol 2020;16(1):11–31.
[43] Le Naour F, Rubinstein E, Jasmin C, Prenant M, Boucheix C. Severely reduced female fertility in CD9-deficient mice. Science 2000;287(5451):319–21.
[44] Zhang J, Dong J, Gu H, Yu S, Zhang X, Gou Y, et al. CD9 is critical for cutaneous wound healing through JNK signaling. J Invest Dermatol 2012;132 (1):226–36.
[45] Aden N, Shiwen X, Aden D, Black C, Nuttall A, Denton CP, et al. Proteomic analysis of scleroderma lesional skin reveals activated wound healing phenotype of epidermal cell layer. Rheumatology (Oxford) 2008;47 (12):1754–60.
[46] Aden N, Nuttall A, Shiwen X, de Winter P, Leask A, Black CM, et al. Epithelial cells promote fibroblast activation via IL-1alpha in systemic sclerosis. J Invest Dermatol 2010;130(9):2191–200.
[47] Nikitorowicz-Buniak J, Shiwen X, Denton CP, Abraham D, Stratton R. Abnormally differentiating keratinocytes in the epidermis of systemic sclerosis patients show enhanced secretion of CCN2 and S100A9. J Invest Dermatol 2014;134(11):2693–702.
[48] Yin J, Liu JS, Feng M, Li JM, Lu S, Yang M, et al. Comprehensively investigating the expression levels and the prognostic role of transforming growth factor beta-induced (TGFBI) in glioblastoma multiforme. Transl Cancer Res 2020;9(10):6487–504.
[49] Figeac N, Mohamed AD, Sun C, Schönfelder M, Matallanas D, Garcia-Munoz A, et al. VGLL3 operates via TEAD1, TEAD3 and TEAD4 to influence myogenesis in skeletal muscle. J Cell Sci 2019;132(13):jcs225946.
[50] Billi AC, Gharaee-Kermani M, Fullmer J, Tsoi LC, Hill BD, Gruszka D, et al. The female-biased factor VGLL3 drives cutaneous and systemic autoimmunity. JCI Insight 2019;4(8):e127291.
[51] Schulz JN, Plomann M, Sengle G, Gullberg D, Krieg T. Eckes B. New developments on skin fibrosis - essential signals emanating from the extracellular matrix for the control of myofibroblasts. Matrix Biol 2018;68-69:522–32.
[52] Wickström SA, Lange A, Montanez E, Fässler R. The ILK/PINCH/parvin complex: the kinase is dead, long live the pseudokinase!. EMBO J 2010;29(2):281–91.
[53] Nüchel J, Ghatak S, Zuk AV, Illerhaus A, Mörgelin M, Schönborn K, et al. TGFB1 is secreted through an unconventional pathway dependent on the autophagic machinery and cytoskeletal regulators. Autophagy 2018;14 (3):465–86.
[54] Perlish JS, Lemlich G, Fleischmajer R. Identification of collagen fibrils in scleroderma skin. J Invest Dermatol 1988;90(1):48–54.